Title

Functional and morphological correlates of developmental dyslexia: A multimodal investigation of the ventral occipitotemporal cortex

Journal

Journal of Neuroimaging, 31(5)

ISSN

1051-2284

Authors

Borghesani, Valentina
Wang, Cheng
Watson, Christa
et al.

Publication Date

2021-09-01

DOI

10.1111/jon.12892

Peer reviewed

Published in final edited form as:

J Neuroimaging. 2021 September ; 31(5): 962–972. doi:10.1111/jon.12892.

Functional and morphological correlates of developmental dyslexia: a multimodal investigation of the ventral occipitotemporal cortex

V. Borghesani[1], **C. Wang**[1,2], **C. Watson**[1,2], **F. Bouhali**[3], **E. Caverzasi**[1,2], **G. Battistella**[1,2], **R. Bogley**[1,2], **N. Yabut**[1,2], **J. Deleon**[1,2], **Z. Miller**[1,2], **F. Hoeft**[3,4], **M-L Mandelli**[1,2], **M-L Gorno-Tempini**[1,2,3]

[1]Department of Neurology, University of California, San Francisco, CA 94158, USA

[2]Dyslexia Center, University of California, San Francisco, CA 94158, USA

[3]Department of Psychiatry and Behavioral Science, and Weill Institute for Neurosciences, UCSF, CA 94158, USA

[4]Department of Psychological Sciences & Brain Imaging Research Center, University of Connecticut, CT 06269, USA

Abstract

Background and Purpose.—The ventral occipitotemporal cortex (vOT) is a region crucial for reading acquisition through selective tuning to printed words. Developmental dyslexia is a disorder of reading with underlying neurobiological bases often associated with atypical neural responses to printed words. Previous studies have discovered anomalous structural development and function of the vOT in individuals with dyslexia. However, it remains unclear if or how structural abnormalities relate to functional alterations.

Methods.—In this study, we acquired structural, functional (words and faces processing), and diffusion MRI data from 26 children with dyslexia (average age 10.4 years ±2.0) and 14 age-matched typically developing readers (average age 10.4 years ±1.6). Morphological indices of local gyrification, neurite density (i.e., dendritic arborization structure), and orientation dispersion (i.e., dendritic arborization orientation) were analyzed within the vOT region that showed preferential activation in typically developing readers for words (as compared to face stimuli).

Results.—The two cohorts diverged significantly in both functional and structural measures. Compared to typically developing controls, children with dyslexia did not show selectivity for words in the left vOT (contrast: words > false fonts). This lack of tuning to printed words was associated with greater neurite dispersion heterogeneity in the dyslexia cohort, but similar neurite density. These group differences were not present in the homologous contralateral area, the right vOT.

[#]Corresponding Author: Maria Luisa Mandelli, Memory and Aging Center - University of California, San Francisco, 675 Nelson Rising Lane, Suite 190 | San Francisco, CA 94158, MariaLuisa.Mandelli@ucsf.edu, (415) 353-2057.

Disclosure

The authors declare no competing financial interests.

Conclusions.—Our findings provide new insight into the neurobiology of the lack of vOT word-tuning in dyslexia by linking behavior, alterations in functional activation and neurite organization.

Keywords

developmental dyslexia; occipitotemporal cortex; functional MRI; diffusion MRI; neurite morphology

INTRODUCTION

Developmental dyslexia (DD) is a neurologically-based learning disorder characterized by reading and spelling difficulties that cannot be explained by differences in general intelligence or education.[1,2,3] DD is the most common learning disorder, impacting 5–10% of school-age children in English-speaking countries and persisting into adulthood.[3,4] While its exact neurobiological basis remains contested, the most consistent finding in brain studies on DD is represented by a functional hypo-activation of a specific region in the left ventral occipitotemporal cortex (vOT) known as the visual word form area (VWFA).[5,6,7] Within the VWFA of typically developing readers, written words elicit higher activation than other visual stimuli[8] such as false-fonts[9] and objects or faces.[10,11] Additionally, sensitivity for letter symbols and whole words is reached as early as 4-years old, whereas specificity requires longer to emerge as suggested by several developmental studies.[12,13,14] Meanwhile, altered vOT activation is consistently found in functional brain studies of DD[15,16] and even in pre-readers at risk for developing DD.[17,18] However, these prior studies had not investigated whether these functional differences in DD relate to structural abnormalities. While the emergence of a functionally tuned vOT region is linked to reading acquisition, it remains to be established if any structural-developmental changes are associated with this process.

Structural anomalies in the language and visual cortices in DD have also been reported, although less consistently than functional differences. Various conventional structural metrics have been investigated, including gray matter volume,[15,19,20,21] cortical thickness,[22,23,24] fractional anisotropy,[25,26] and gyrification.[24,27] Moreover, rare postmortem case studies have found neurobiological alterations in DD, particularly in areas of focal cortical dysgenesis in left perisylvian regions, suggestive of neuronal migrational abnormalities.[28,29,30,31,32]

Molecular genetic studies using animal models have associated developmental anomalies with anomalies of axon guidance as well as dendrite growth and differentiation.[33,34,35] Yet, only a few studies so far have examined abnormalities of neurite (i.e., axon and dendrite) morphology in individuals with DD, partially due to the technical limitations of imaging and quantifying neurite properties in vivo. A relatively novel technique, neurite orientation dispersion and density imaging (NODDI), can provide metrics more specific to brain tissue microstructure, compared to the traditional diffusion tensor imaging techniques.[36] By applying a three-compartment model to multi-shell diffusion MRI (dMRI) data, NODDI provides a solution to inferring tissue microstructure traits, including neurite density and orientation dispersion. Therefore, it is considered to be well-suited in capturing dendritic and

axonal architecture in gray matter, allowing one to relate neuronal properties to functional differences.[37] Only one study so far has examined in-vivo neurite morphology in individuals with DD using NODDI.[27]

Here, we investigated functional and structural features of the vOT in children diagnosed with DD (hereafter DYS) compared to age-matched, typically-developing controls (hereafter TDC). First, we compared activation patterns associated with word and face stimuli to identify the regions of the vOT tuned to words and faces in TDC and characterize their differences in DD. Then, we examined neurite morphology of those regions of the vOT in both cohorts. Given the association of DD susceptibility genes with neurite abnormalities, we hypothesized that reduced activation in the vOT for words would be linked to morphological differences, such as lower neurite density and less orientation coherence in DYS.

METHODS

Participants

Right-handed, native English-speaking children were recruited through the University of California San Francisco (UCSF) Dyslexia Center, a multidisciplinary research center dedicated to the study of dyslexia and neurodevelopmental cognitive disorders. Guardians of the participants provided informed written consent and participants provided assent. The study was approved by the UCSF Institutional Review Board and complied with the declaration of Helsinki. For the children in the DD cohort (DYS, n=26, 14 female, average age 10.4 years ±2.0), inclusion criteria required a previous diagnosis of DD. Exclusion criteria included all objective reading scores at the time of study falling above the 25th percentile of same-aged peers (which represents the start of the average range), general cognitive scores [Wechsler Abbreviated Scale of Intelligence (WASI) Matrix Reasoning] that fell below the 9th percentile of same-aged peers, an acquired brain injury, or genetic or psychiatric disorder associated with impaired sensory processing or communication, and contraindications for MRI. Their reading difficulties persisted despite appropriate schooling in an establishment with specific reading interventions in small classes. For typically developing children (TDC, n=14, 5 female, average age 10.4 years ±1.6), exclusion criteria were any single word reading scores falling below the 16th percentile of same-aged peers (which is equivalent to −1 standard deviation), any history of developmental delays, and contraindications for MRI. Table 1 reports the demographic and neuropsychological characteristics of the sample. Participants were assessed with standard neuropsychological and academic batteries (see below).

Neuropsychological and Academic Assessment

Neuropsychological and academic assessments were administered either by a neuropsychologist, or a member of staff trained and supervised by neuropsychologists. Neuropsychological testing covered screening of nonverbal reasoning (WASI Matrix Reasoning). Academic performance was assessed using the timed Test of Word Reading Efficiency – Second Edition (TOWRE-2)[38] which includes Sight Word Efficiency (SWE) for timed single-word reading of real words and Phonemic Decoding Efficiency (PDE)

for timed single-word reading of pseudowords. Additionally, the Gray Oral Reading Test (GORT-5)[39] was used to evaluate paragraph reading. Due to time limitations, protocol updates, or subject fatigue, not all DYS participants were able to complete all of the tests (see Table 1).

Imaging Data Acquisition

All neuroimaging data were acquired using a 3T Siemens Trio scanner (Siemens, Erlangen, Germany) equipped with a 12-channel phased-array head coil at the Neuroimaging Center of UCSF. Head movement was minimized by stabilizing the head with cushions. It is well known that head motion presents a challenge in fMRI studies, especially in pediatric populations. For this reason, we allowed our participants to take a break every 20 minutes, a procedure that has proved to reduce head motion during functional data acquisition.[40] Metrics about head motion were calculated from the translational and rotational parameters of the rigid correction of the head motion: 1) the maximum absolute translation of each brain volume as compared to the previous volume (maximum motion), 2) the mean absolute displacement of each brain volume as compared to the previous volume (mean motion), 3) the average of the absolute value of the Euler angle of the rotation of each brain volume as compared to the previous volume (rotation), and 4) the framewise displacement (FD) that measures the movement of any given frame relative to the previous frame.[41] The thresholds for each of these types of motion used as criteria for exclusion were the following: maximum translation at 2 mm, maximum rotation at 2 degrees, and FD less than 0.5 mm for every volume.

Functional MRI parameters and design—Functional data were collected with a single-shot echo planar imaging sequence with the following acquisition parameters: repetition time (TR) / echo-time (TE) = 2000/31 ms; flip angle = 80°; imaging parallel acceleration factor (iPAT) = 2; number of axial slices = 32; in plane voxel size = 2.4 × 2.4 mm^2; slice thickness = 3.6 mm; Field of View (FOV) = 230 × 230 mm^2; multi-slice mode = interleaved ascending.

While in the scanner, participants performed two tasks: a word task (to assess ventral occipitotemporal cortex (vOT) responses to printed words), followed by a face task (to assess vOT responses to faces, another meaningful visual category). During the word task, we presented six 20-second blocks of real words and six 20-second blocks of false fonts (23 trials/block; 370 ms stimulus presentation and 500 ms inter-stimulus), interleaved with six blocks of 20-second fixation. Participants were instructed to fixate at the center of the screen throughout the task and press a button using the right thumb every time a stimulus appeared in red presented pseudo-randomly (4 times over the six-word blocks and 4 times over the 6 false font blocks). Similarly, during the face task, cartoon faces and scrambled images were presented interleaved with fixation blocks. Participants pressed a button every time they saw a blank oval image instead of a cartoon face or a scrambled image (4 times over the six face blocks and 4 times over the 6 scrambled blocks). Examples of the stimuli and time-course of the experimental paradigm are illustrated in Fig. 1. As described by Wilson and colleagues,[42] the word stimuli were 6-letter-long nouns and adjectives of medium frequency extracted from Coltheart (1981)[43] while the false font stimuli were strings of 6

letters in a non-Roman alphabet. Cartoon faces from popular children's shows were selected from public websites, converted to grayscale pictures, and framed with a black oval mask to avoid background interferences. Finally, scrambled images were generated matching the intensity of the cartoon faces. All stimuli were presented with Psychtoolbox-3 (http://psychtoolbox.org) running on Matlab R2016b (http://www.mathworks.com). Participants received appropriate training outside the scanner to familiarize them with the stimuli and task.

Structural MRI acquisition—Anatomical images were acquired with a 3D T1-weighted sagittal Magnetization Prepared Rapid Acquisition Gradient Echo (MPRAGE) sequence with the following acquisition parameters: 160 sagittal slices, TR/TE = 2300/2.98 ms; flip angle = 9°; voxel size = 1 × 1 × 1 mm^3; FOV = 256 × 240 mm^2; iPAT = 2.

Axial multi-shell diffusion MRI (dMRI) was acquired with 64 directions at b=2000 s/mm^2, and with 30 directions at b=700 s/mm^2, phase encoding direction = anterior-posterior, TR/TE = 8200/86 ms, in-plane voxel size = 2.2 × 2.2 mm^2, slice thickness = 2.2 mm; FOV = 220 × 220 mm^2, 60 contiguous slices, flip angle = 9°, iPAT = 2, including 10 volumes without diffusion-weighting (b0 images), one of which was acquired using a reversed phase-encoding direction (posterior to anterior). The latter allowed estimation and correction for susceptibility-induced distortions. The total acquisition time of the dMRI data was approximately 15 min. While MRI and fMRI data are available in all children, dMRI was only acquired in a subsample of 31 children (17 DYS, 14 TDC).

Imaging Data Preprocessing and Analysis

Functional MRI processing and statistical analysis—Functional data were processed using SPM12 (Wellcome Department of Cognitive Neurology, London, UK, http://www.fil.ion.ucl.ac.uk). The functional images underwent field map correction, realignment to the first volume, normalization to the Montreal Neurological Institute (MNI) space, and smoothing with a full width at half maximum (FWHM) of a 5 mm isotropic Gaussian kernel.

After preprocessing, activations in response to each condition (i.e., words and false fonts in the word task, faces and scrambled pictures in the face task) were estimated for each participant using the standard general linear model (GLM) with a high-pass filter with a cut-off frequency at 1/128 Hz and corrected for temporal autocorrelation with an AR(1) model. This first level model included separate regressors for each experimental condition convolved with a canonical hemodynamic response function, as well as six motion covariates modeling head translation and rotation. Word selectivity was defined using the contrast: words > false fonts, while face selectivity was defined by the contrast: faces > scrambled images.

First, statistical analyses were performed to identify regions that responded selectively to words (and separately to faces) in TDC and DYS, with age and sex as covariates. Using one GLM for both groups allowed isolation of selectivity effects and group effects (TDC > DYS). In Figure 2, plotted clusters are set at a threshold of $p < 0.001$ uncorrected with a

cluster extent threshold of 100 voxels. Table 2 reports those surviving cluster-wise control of family-wise error at $p < 0.05$.

Then, to examine the relationship between vOT word selectivity and reading efficiency, we correlated the participants' neural responses (BOLD activation) in the TDC vOT region tuned to words (see below) with raw scores on the timed real word (SWE) and pseudoword reading (PDE).

Structural MRI processing—The T1 structural images were preprocessed using FreeSurfer version 5.3 (http://surfer.nmr.mgh.harvard.edu/).[44,45,46] A trained neuroradiologist (EC) visually inspected the segmentation results. Cortical parcellation and thickness measurements were performed by using the Desikan-Killiany Atlas comprising 34 cortical volumes of interest per hemisphere.[47] Gyrification of the entire cortex was also assessed using Freesurfer. The 3-D local gyrification index (lGI) was computed using the method described by Schaer and colleagues.[48,49] A study-specific template was created based on all subjects and the FreeSurfer dataset was resampled to the average space.[49] The results were smoothed with a FWHM of 5 mm for lGI.

Diffusion MRI processing—Diffusion MRI data were preprocessed and analyzed to extract neurite morphological features. During preprocessing, the susceptibility-induced off-resonance field for each participant was estimated from a pair of images acquired with reversed phase-encoding directions. The distortion estimation and correction were performed using the top-up tool of FMRIB Software Library (FSL).[50] Additionally, eddy current-induced distortion and head motion were corrected using eddy_correct from the same toolbox; b-vectors were rotated accordingly to account for the corrections.

The NODDI model was applied to the preprocessed dMRI data using a toolbox developed in Matlab (http://mig.cs.ucl.ac.uk/). The model decomposes the signal from each voxel into three compartments (extra-neurite, intra-neurite, and isotropic Gaussian diffusion) and provides metrics more specific to the microstructure brain architecture, such as neurite density index (NDI) and orientation dispersion index (ODI). NDI is related to the amount of neurites, and possible proxy for myelination, axonal growth or greater axonal density, while ODI is related to the degree of dispersion of the neurites thus a more geometrical proxy.[36]

Structural analyses of vOT region tuned to words—Based on the fMRI group activation pattern in the contrast words > false fonts in the TDC cohort only (hereafter: TDC-VWFA), we identified the targeted occipitotemporal ROI in MNI space. We then transformed the ROI into a "label" in Freesurfer: we used the QDEC application to back-project the ROI into each single-subject T1 space to extract the mean lGI value on the cortical surface. To extract metrics of ODI and NDI in the functional ROI in each participant, we used linear (bbregister, https://surfer.nmr.mgh.harvard.edu/fswiki/bbregister) and nonlinear transformations implemented in Freesurfer to map the functional region in the MNI space in each subject's diffusion space. These steps allowed comparisons between the two cohorts of their micro- and macro- structural characteristics, namely ODI, NDI, and lGI. For each metric, we performed a generalized linear model looking for a main effect of the cohorts, sex, and age, as well as their interactions.

RESULTS

Demographic and neuropsychological profiles

There were no significant differences in age, sex, or non-verbal intelligence score (WASI Matrix Reasoning) between children with developmental dyslexia and typically developing controls (all p's > 0.25). As expected, the groups differed in TOWRE scores, with DYS showing significantly lower scores than TDC in both subtests (p's < 0.001). Demographics, oral language scores, and other neuropsychological measures are reported in Table 1.

Functional MRI activation patterns

Based on the head-motion exclusion criteria, face-task data from three DYS children were excluded from further analyses.

Group-level whole-brain analyses in TDC revealed a left-lateralized functional cluster of activation in the vOT area selectively tuned to printed words (contrast: words > false fonts; cluster hereafter referred to as TDC-VWFA). Additionally, the left inferior frontal gyrus (IFG), middle frontal gyrus (MFG), and precentral gyrus showed significantly more activation in the words condition than the false fonts condition (Fig. 2, upper left). In the cohort of children with DYS, the same contrast did not lead to any statistically significant result (Fig. 2, middle-left).

The contrast of faces > scrambled images revealed a large bilateral set of functional activations in vOT regions qualitatively similar between the TDC and DYS groups (Fig. 2, rightmost column).

As expected, a direct group comparison of the two cohorts for the contrast of words > false fonts revealed reduced activation in the left fusiform gyrus in DYS. Additionally, DYS showed reduced word selectivity in the left IFG, MFG, angular gyrus, and superior parietal lobule compared to TDC (Figure 2, Table 2). The direct group comparison TDC > DYS for face selectivity revealed reduced activation only in small portions of the posterior right fusiform gyrus in DYS, in line with previous reports.[51] No clusters appeared for DYS > TDC for either word or face selectivity.

We examined the relationship between word selectivity in the TDC-VWFA cluster and rapid single-word reading performance. A positive correlation across all children between TDC-VWFA activation and raw scores of both SWE ($r = 0.76$, $p < 0.001$) and PDE ($r = 0.56$, $p = 0.001$) indicates an association between tuning for printed words and reading efficiency of both words and pseudowords (Fig.3a).

The word selectivity region isolated by the contrast words > false fonts in the TDC cohort appears to be near the typical visual word form area (VWFA) coordinates (e.g., [x=−44 y=−58 z=−15] identified in a meta-analysis by Jobard and colleagues.[52] As this contrast revealed no significant cluster in the DYS group, and given the proximity to previously reported VWFA coordinates, we used these peak coordinates in our TDC group to define our region of interest for following morphological analyses.

Structural and morphological findings

Three metrics were used to compare structural and morphological features of the VWFA in TDC and children with DYS: neurite orientation dispersion (i.e., ODI), neurite density (i.e., NDI), and local gyrification indices (i.e., lGI).

Analysis of neurite ODI in the left TDC-VWFA revealed a significant group effect ($F = 5.57$, $p = 0.02$) with DYS showing greater ODI (i.e., less coherence) than TDC (Fig. 3b). There was no main effect of age or gender, and no interaction. Similar comparisons of the NDI did not show any main effect nor interaction. The same was true for the cortical folding analysis (i.e., lGI).

Finally, for all three morphological metrics, the control analyses in the right homologue of the TDC-VWFA revealed no significant effects.

DISCUSSION

In this study, we capitalized on multimodal imaging to investigate functional and morphological correlates of the ventral occipitotemporal cortex in children with developmental dyslexia. Compared to typically developing readers, children with DD showed less tuning for printed words in the left vOT. Crucially, the observed alteration in functional tuning in DYS was associated with neuronal morphological differences, namely lower neurite orientation coherence (i.e., greater ODI in DYS). Taken together, our results suggest that neuronal structure and function of the vOT would be able to dissociate DYS from TDC, and thus have important implications for current neurocognitive models of reading as well as clinical and research efforts in DD.

DD and vOT functional activations: *weaker tuning to words*

Children with DD showed reduced tuning to printed words in the left VWFA within the vOT as compared to TDC children. Moreover, the results of the face task indicate a comparable response in terms of topography and strength in TDC and DYS in the left vOT, suggesting that the weaker tuning for words in DD is specific and cannot be ascribed to a generalized deficit of activation/specialization in the vOT. Hence, our fMRI findings speak to the pivotal role played by the VWFA in linking the behavioral and neural characteristics of DD.

Our results are in line with numerous previous studies suggesting a key role of vOT functional abnormalities in DD.[6,53] The coupling of reduced word-selectivity in the left fusiform and reduced face selectivity in the right fusiform in DYS has been previously interpreted as evidence of altered resolution of the competition between the representations of words and that of faces in the vOT.[51] As corroborated by our findings, children with DD appear to show not only hypoactivation,[54] but also atypical neural tuning along the vOT: their response profile lacks the typical posterior-to-anterior gradient (i.e., higher anterior activity for letters, higher posterior activity for false-fonts) and fails to show sensitivity to orthographic familiarity (i.e., increased activity for unfamiliar letter strings compared to familiar letter strings).[7,55,56] The nested representational hierarchy of visual information supported by the vOT[57] undergoes a prolonged maturation,[58] after which different populations of neurons appear to be tuned to ecologically relevant categories (e.g., faces,

tools). The development of an area selectively tuned to words, a phylogenetically recent human invention, appears to require a longer time to mature.[12,13,14] The complex series of changes required to associate arbitrary cultural symbols to a specific and reproducible cerebral substrate,[59] seems to fail in DD. One could speculate that this functional alteration is due to morphological aspects stemming from genetic differences.[18,60,61,62] The observed atypical tuning for words would thus be the downstream effect of a structurally vulnerable vOT. On the other hand, a ready-to-be-molded vOT could fail to develop proper selectivity for printed stimuli as a function of altered experiences during reading acquisition. A critical factor could be the lack of proper inputs from brain regions encoding semantic and phonological representations, such as the anterior temporal lobe and the parietal/superior temporal cortex respectively. For instance, previous studies have shown that recruitment of the visual word form area (VWFA) during non-reading tasks is absent in children with DD, supporting an impaired influence of phonological representations,[63] adding to the open debate on the nature and prominence of top-down inputs on the VWFA.[64,65] Overall, the VWFA is connected, via short- and long-range white matter tracts, to widespread regions in language networks,[66,67,68,] acting as a critical hub for the integration of orthographic, phonological and semantic representations.

These structural (and functional) connections can explain the observation that the left vOT is not the only area where TDC showed greater word-specific activation than DYS. A similar pattern was observed in the left inferior frontal gyrus and angular gyrus, two cortical regions of the dorsal language network that, respectively, associate with articulatory-phonological and semantic processing.[69,70] Our finding could thus be explained by a more automatic orthography-to-phonology mapping, heightened subvocal rehearsal, and/or faster semantic retrieval in typical readers.[71] Coherently, previous studies have found hypoactivation of left inferior parietal and hyperactivation of left inferior frontal cortices in DD.[72] Moreover, changes in effective connectivity between vOT and inferior frontal gyrus (IFG) have been associated with reading development and shown to be altered in DD.[73] Further studies, focusing on these dorsal areas and their contribution to behavioral performance, will elucidate their relationship with the ventral effects we focus on here.

Overall, our functional results are in line with previous literature in indicating hypoactivation in vOT as a neural correlate of DD.[6,74] While we cannot resolve the debate on whether this lack of tuning to printed words is the cause or rather the consequences of the reading deficit, we show that this functional abnormality directly relates not only to behavioral performance but also to morphological differences.

DD and vOT structural morphology: *similar neurite density yet less orientation coherence*

Compared to typical readers, children with DD showed less orientation coherence (i.e., higher ODI) in the left vOT, while neurite density did not show a group difference. Previous studies have indicated that cortical orientation dispersion is associated with the proportion of tangential fibers vs. radial fibers.[75,76] Our results thus suggest that abnormal function of left vOT in DD is associated with a disorganization of the neurite architecture rather than with altered cortical myelination.

In our sample, TDC and DYS did not statistically differ in terms of cortical folding (i.e., lGI). This finding is at odds with previous studies associating DD with vOT atypical sulcal patterns,[77] reduced cortical thickness, and increased gyrification.[24] Our group has previously reported the absence of typical lGI age-related decrease in language-related left frontotemporal regions in children with DD.[27] A decrease in lGI is considered an important feature of cerebral cortex development,[78] enhancing neural efficiency by improving communications. In particular, it may reflect the need of developing extensive long-range connections, critical for widespread neurocognitive networks such as language ones. Hence, increased gyrification in DD could reflect reduced long-range connectivity among reading-related hubs. The complex interaction between lGI differences and neurite density/coherence suggests that gyrification and neurite organization are related yet affect specific regions in selective ways.

Our structural analyses focused on gray matter differences, but the contribution of white matter tracts to brain development cannot be overlooked.[79] Critically, both structural and functional studies have demonstrated VWFA preferential connectivity with language areas[66,80] , and recent studies of white matter suggest that neurite density and dispersion are sensitive to unique developmental features.[81] Taken together, these findings call for deeper investigations of the microstructural features of white matter in DD.

Overall, our results corroborate the idea that neuromorphological differences are one of the core elements of DD, emphasizing the importance of disentangling the specific contributions of gyrification, neurite density, and neurite orientation dispersion. As discussed for the functional results, it remains to be seen to what extent these neuromorphological differences are set at birth (i.e., genetically predetermined) or rather if they develop in the first years of life during formal reading education (i.e., resulting from experience-dependent brain changes). Volumetric indexes, known to be affected by postnatal changes,[82] are altered in DD before reading onset.[83] Yet, the global pattern of gyri and sulci is thought to be prenatally determined, showing little change during postnatal development.[84,85] Thus, a focus on neuromorphological indices measured with multi-compartment diffusion models, paired with a longitudinal empirical design, will provide better insights.

Limitations

The neurobiological and genetic bases of DD are well-accepted,[86] yet the field also acknowledges that DD is a behaviorally, functionally, and structurally multifaceted product of interacting biological and environmental causes changing over time.[87] While our study examined a cross-sectional sample, longitudinal designs will shed light on the timing and directionality of the relationship between behavioral, functional, and morphological aspects of DD.[88] Overall, longitudinal multimodal studies with appropriate stratification of DD clinical phenotypes will have the potential to resolve current inconsistencies in DD research and provide etiological explanations.[53,89,90] The interpretation of the NODDI metrics considered in this study need to be taken with caution. Although the NODDI model introduced more specific metrics of the micro-structural complexity of the brain tissues and for both white and gray matter compared to the standard DTI metrics, and increasing histopathological evidences reasonably relates NDI and ODI to histologically match neurite

density and orientation dispersion[75], this model still faces important limitations: the oversimplification of the model that is currently under debate[91.92,93] and the diffusion image resolution that is still far distant from the anatomical neurite resolution. To overcome these limitations, improved methodologies for diffusion MRI, such as NODDI with diffusivity assessment (NODDIDA)[92] and spherical mean technique (SMT)[93] are being developed and will be considered in future implementations of the MRI protocol.

Finally, our sample size prevents more robust analyses of the relationship between behavioral performance, functional and morphological differences, warranting future studies with larger sample sizes. For instance, what is likely a mild sampling bias in our controls cohort leads to a small, not significant, difference in the WASI Matrix reasoning score of the two groups. However, given that the groups were not significantly different this potential bias is unlikely to account for the group differences found in the imaging analyses.

Conclusion

Our study showed associations between behavioral (i.e., impaired reading performance), functional (i.e., altered neural tuning), and neuromorphological (i.e., less coherent neurite orientation) features of DD. These findings inform current reading models by highlighting the critical role of the left vOT cortex in the pathophysiology of DD. Efficient reading appears to be critically linked with the development of appropriate functional tuning of the left posterior vOT, the gateway between the ventral and dorsal language networks. Thus, we underscore how multimodal imaging will be pivotal in capturing neurobiologically coherent phenotypes within the umbrella definition of developmental dyslexia.

Acknowledgements

The authors thank the participants and their families for the time and effort they dedicated to the research. This research was supported by the Charles and Helen Schwab Foundation. Dr. Gorno Tempini was supported by the National Institute of Health (NINDS R01 NS050915; NIDCD K24 DC015544; NIA P01 AG019724; NIA P50 AG023501).

References

1. Lyon GR, Shaywitz SE, Shaywitz BA. A definition of dyslexia. Ann of Dyslexia 2003;53:1–14.
2. Peterson RL, Pennington BF. Developmental dyslexia. Annu Rev Clin Psychol 2015;11:283–307. [PubMed: 25594880]
3. Schulte-Körne G The prevention, diagnosis, and treatment of dyslexia. Dtsch Arztebl Int 2010;107:718–26 [PubMed: 21046003]
4. Cavalli E, Colé P, Leloup G, Poracchia-George F, Sprenger-Charolles L, El Ahmadi A. Screening for dyslexia in french-speaking university students: An evaluation of the detection accuracy of the Alouette test. J Learn Disabil 2018;51:268–82. [PubMed: 28423976]
5. Martin A, Kronbichler M, Richlan F. Dyslexic brain activation abnormalities in deep and shallow orthographies: A meta-analysis of 28 functional neuroimaging studies. Hum Brain Mapp 2016;37:2676–99. [PubMed: 27061464]
6. Richlan F, Kronbichler M, Wimmer H. Meta-analyzing brain dysfunctions in dyslexic children and adults. Neuroimage 2011;56:1735–42. [PubMed: 21338695]
7. van der Mark S, Bucher K, Maurer U, et al. Children with dyslexia lack multiple specializations along the visual word-form (VWF) system. Neuroimage 2009;47:1940–9. [PubMed: 19446640]

8. Cohen L, Lehéricy S, Chochon F, Lemer C, Rivaud S, Dehaene S. Language-specific tuning of visual cortex? Functional properties of the visual word form area. Brain 2002;125:1054–69. [PubMed: 11960895]
9. Vinckier F, Dehaene S, Jobert A, Dubus JP, Sigman M, Cohen L. Hierarchical coding of letter strings in the ventral stream: dissecting the inner organization of the visual word-form system. Neuron 2007;55:143–56. [PubMed: 17610823]
10. Gauthier I, Tarr MJ, Moylan J, Skudlarski P, Gore JC, Anderson AW. The fusiform "face area" is part of a network that processes faces at the individual level. J Cogn Neurosci 2000;12:495–504. [PubMed: 10931774]
11. Hasson U, Levy I, Behrmann M, Hendler T, Malach R. Eccentricity bias as an organizing principle for human high-order object areas. Neuron 2002;34:479–90. [PubMed: 11988177]
12. Cantlon JF, Pinel P, Dehaene S, Pelphrey KA. Cortical representations of symbols, objects, and faces are pruned back during early childhood. Cereb Cortex 2011;21:191–9. [PubMed: 20457691]
13. Centanni TM, King LW, Eddy MD, Whitfield-Gabrieli S, Gabrieli JDE. Development of sensitivity versus specificity for print in the visual word form area. Brain Lang 2017;170:62–70. [PubMed: 28411527]
14. Olulade OA, Flowers DL, Napoliello EM, Eden GF. Developmental differences for word processing in the ventral stream. Brain Lang 2013;125:134–45. [PubMed: 22564748]
15. Linkersdörfer J, Lonnemann J, Lindberg S, Hasselhorn M, Fiebach CJ. Grey matter alterations co-localize with functional abnormalities in developmental dyslexia: an ALE meta-analysis. PLoS One 2012;7:e43122. [PubMed: 22916214]
16. Richlan F, Kronbichler M, Wimmer H. Functional abnormalities in the dyslexic brain: a quantitative meta-analysis of neuroimaging studies. Hum Brain Mapp 2009;30:3299–308. [PubMed: 19288465]
17. Specht K, Hugdahl K, Ofte S, et al. Brain activation on pre-reading tasks reveals at-risk status for dyslexia in 6-year-old children. Scand J Psychol 2009;50:79–91. [PubMed: 18826418]
18. Vandermosten M, Hoeft F, Norton ES. Integrating MRI brain imaging studies of pre-reading children with current theories of developmental dyslexia: A review and quantitative meta-analysis. Curr Opin Behav Sci 2016;10:155–161. [PubMed: 27458603]
19. Kronbichler M, Wimmer H, Staffen W, Hutzler F, Mair A, Ladurner G. Developmental dyslexia: gray matter abnormalities in the occipitotemporal cortex. Hum Brain Mapp 2008;29:613–25. [PubMed: 17636558]
20. Richlan F, Kronbichler M, Wimmer H. Structural abnormalities in the dyslexic brain: a meta-analysis of voxel-based morphometry studies. Hum Brain Mapp 2013;34:3055–65. [PubMed: 22711189]
21. Silani G, Frith U, Demonet JF, et al. Brain abnormalities underlying altered activation in dyslexia: a voxel based morphometry study. Brain 2005;128:2453–61. [PubMed: 15975942]
22. Altarelli I, Monzalvo K, Iannuzzi S, et al. A functionally guided approach to the morphometry of occipitotemporal regions in developmental dyslexia: evidence for differential effects in boys and girls. J Neurosci 2013;33:11296–301. [PubMed: 23825432]
23. Clark KA, Helland T, Specht K, et al. Neuroanatomical precursors of dyslexia identified from pre-reading through to age 11. Brain 2014;137:3136–41. [PubMed: 25125610]
24. Williams VJ, Juranek J, Cirino P, Fletcher JM. Cortical thickness and local gyrification in children with developmental dyslexia. Cereb Cortex 2018;28:963–73. [PubMed: 28108497]
25. Niogi SN, McCandliss BD. Left lateralized white matter microstructure accounts for individual differences in reading ability and disability. Neuropsychologia 2006;44:2178–88. [PubMed: 16524602]
26. Vandermosten M, Boets B, Wouters J, Ghesquière P. A qualitative and quantitative review of diffusion tensor imaging studies in reading and dyslexia. Neurosci Biobehav Rev 2012;36:1532–52. [PubMed: 22516793]
27. Caverzasi E, Mandelli ML, Hoeft F, et al. Abnormal age-related cortical folding and neurite morphology in children with developmental dyslexia. Neuroimage Clin 2014;18:814–21.
28. Galaburda AM, Sherman GF, Rosen GD, Aboitiz F, Geschwind N. Developmental dyslexia: four consecutive patients with cortical anomalies. Ann Neurol 1985;18:222–33. [PubMed: 4037763]

29. Galaburda AM, Kemper TL. Cytoarchitectonic abnormalities in developmental dyslexia: a case study. Ann Neurol 1979;6:94–100. [PubMed: 496415]
30. Humphreys P, Kaufmann WE, Galaburda AM. Developmental dyslexia in women: neuropathological findings in three patients. Ann Neurol 1990;28:727–38. [PubMed: 2285260]
31. Miller ZA, Spina S, Pakvasa M, et al. Cortical developmental abnormalities in logopenic variant primary progressive aphasia with dyslexia. Brain Commun 2019;1:fcz027. [PubMed: 32699834]
32. Guidi LG, Velayos-Baeza A, Martinez-Garay I, et al. The neuronal migration hypothesis of dyslexia: A critical evaluation 30 years on. Eur J Neurosci 2018;48:3212–33. [PubMed: 30218584]
33. Hannula-Jouppi K, Kaminen-Ahola N, Taipale M, et al. The axon guidance receptor gene ROBO1 is a candidate gene for developmental dyslexia. PLoS Genet 2005;1:e50. [PubMed: 16254601]
34. Peschansky VJ, Burbridge TJ, Volz AJ, et al. The effect of variation in expression of the candidate dyslexia susceptibility gene homolog Kiaa0319 on neuronal migration and dendritic morphology in the rat. Cereb Cortex 2010;20:884–97. [PubMed: 19679544]
35. Scerri TS, Schulte-Körne G. Genetics of developmental dyslexia. Eur Child Adolesc Psychiatry 2010;19:179–97. [PubMed: 20091194]
36. Zhang H, Schneider T, Wheeler-Kingshott CA, Alexander DC. NODDI: practical in vivo neurite orientation dispersion and density imaging of the human brain. Neuroimage 2012;61:1000–16. [PubMed: 22484410]
37. Jespersen SN, Bjarkam CR, Nyengaard JR, et al. Neurite density from magnetic resonance diffusion measurements at ultrahigh field: comparison with light microscopy and electron microscopy. Neuroimage 2010;49:205–16. [PubMed: 19732836]
38. Torgesen JK, Wagner RK, Rashotte CA. Test of word recognition efficiency Austin, TX: Pro-Ed; 1999.
39. Wiederholt JL, Bryant BR. Gray oral reading tests: GORT-3 Austin, TX: Pro-ed; 1992.
40. Meissner TW, Walbrin J, Nordt M, Koldewyn K, Weigelt S. Head motion during fMRI tasks is reduced in children and adults if participants take breaks. Dev Cogn Neurosci 2020;44:100803. [PubMed: 32716852]
41. Power JD, Barnes KA, Snyder AZ, Schlaggar BL, Petersen SE. Spurious but systematic correlations in functional connectivity MRI networks arise from subject motion. Neuroimage 2012;59:2142–54. [PubMed: 22019881]
42. Wilson SM, Rising K, Stib MT, Rapcsak SZ, Beeson PM. Dysfunctional visual word form processing in progressive alexia. Brain 2013;136:1260–73. [PubMed: 23471694]
43. Coltheart M The MRC psycholinguistic database. Q J Exp Psychol A 1981;33:497–505.
44. Dale AM, Fischl B, Sereno MI. Cortical surface-based analysis. I. Segmentation and surface reconstruction. Neuroimage 1999;9:179–94. [PubMed: 9931268]
45. Fischl B, Sereno MI, Dale AM. Cortical surface-based analysis. II: Inflation, flattening, and a surface-based coordinate system. Neuroimage 1999;9:195–207. [PubMed: 9931269]
46. Fischl B, Sereno MI, Tootell RB, Dale AM. High-resolution intersubject averaging and a coordinate system for the cortical surface. Hum Brain Mapp 1999;8:272–84. [PubMed: 10619420]
47. Desikan RS, Ségonne F, Fischl B, et al. An automated labeling system for subdividing the human cerebral cortex on MRI scans into gyral based regions of interest. Neuroimage 2006;31:968–80. [PubMed: 16530430]
48. Schaer M, Cuadra MB, Tamarit L, Lazeyras F, Eliez S, Thiran JP. A surface-based approach to quantify local cortical gyrification. IEEE Trans Med Imaging 2008;27:161–70. [PubMed: 18334438]
49. Schaer M, Cuadra MB, Schmansky N, Fischl B, Thiran JP, Eliez S. How to measure cortical folding from MR images: a step-by-step tutorial to compute local gyrification index. J Vis Exp 2012;59:e3417.
50. Smith SM, Jenkinson M, Woolrich MW, et al. Advances in functional and structural MR image analysis and implementation as FSL. Neuroimage 2004;23 (Suppl 1):S208–19. [PubMed: 15501092]

51. Monzalvo K, Fluss J, Billard C, Dehaene S, Dehaene-Lambertz G. Cortical networks for vision and language in dyslexic and normal children of variable socio-economic status. Neuroimage 2012;61:258–74. [PubMed: 22387166]
52. Jobard G, Crivello F, Tzourio-Mazoyer N. Evaluation of the dual route theory of reading: a metanalysis of 35 neuroimaging studies. Neuroimage 2003;20:693–712. [PubMed: 14568445]
53. Kronbichler L, Kronbichler M. The importance of the left occipitotemporal cortex in developmental dyslexia. Curr Dev Disord Rep 2018;5:1–8. [PubMed: 29497594]
54. Paz-Alonso PM, Oliver M, Lerma-Usabiaga G, et al. Neural correlates of phonological, orthographic and semantic reading processing in dyslexia. Neuroimage Clin 2018;20:433–47. [PubMed: 30128282]
55. Olulade OA, Flowers DL, Napoliello EM, Eden GF. Dyslexic children lack word selectivity gradients in occipito-temporal and inferior frontal cortex. Neuroimage Clin 2015;7:742–54. [PubMed: 25844326]
56. Wimmer H, Schurz M, Sturm D, et al. A dual-route perspective on poor reading in a regular orthography: an fMRI study. Cortex 2010;46:1284–98. [PubMed: 20650450]
57. Grill-Spector K, Weiner KS. The functional architecture of the ventral temporal cortex and its role in categorization. Nat Rev Neurosci 2014;15:536–48. [PubMed: 24962370]
58. Golarai G, Ghahremani DG, Whitfield-Gabrieli S, et al. Differential development of high-level visual cortex correlates with category-specific recognition memory. Nat Neurosci 2007;10:512–22. [PubMed: 17351637]
59. Dehaene S, Cohen L. Cultural recycling of cortical maps. Neuron 2007;56:384–98. [PubMed: 17964253]
60. Skeide MA, Kraft I, Müller B, et al. NRSN1 associated grey matter volume of the visual word form area reveals dyslexia before school. Brain 2016;139:2792–803. [PubMed: 27343255]
61. Cachia A, Roell M, Mangin JF, et al. How interindividual differences in brain anatomy shape reading accuracy. Brain Struct Funct 2018;223:701–12. [PubMed: 28916842]
62. Beelen C, Vanderauwera J, Wouters J, Vandermosten M, Ghesquière P. Atypical gray matter in children with dyslexia before the onset of reading instruction. Cortex 2019;121:399–413. [PubMed: 31704534]
63. Desroches AS, Cone NE, Bolger DJ, Bitan T, Burman DD, Booth JR. Children with reading difficulties show differences in brain regions associated with orthographic processing during spoken language processing. Brain Res 2010;1356:73–84. [PubMed: 20691675]
64. Dehaene S, Cohen L, Sigman M, Vinckier F. The neural code for written words: a proposal. Trends Cogn Sci 2005;9:335–41. [PubMed: 15951224]
65. Price CJ, Devlin JT. The interactive account of ventral occipitotemporal contributions to reading. Trends Cogn Sci 2011;15:246–53. [PubMed: 21549634]
66. Bouhali F, Thiebaut de Schotten M, Pinel P, et al. Anatomical connections of the visual word form area. J Neurosci 2014;34:15402–14. [PubMed: 25392507]
67. Moulton E, Bouhali F, Monzalvo K, et al. Connectivity between the visual word form area and the parietal lobe improves after the first year of reading instruction: a longitudinal MRI study in children. Brain Struct Funct 2019;224:1519–36. [PubMed: 30840149]
68. Yeatman JD, Rauschecker AM, Wandell BA. Anatomy of the visual word form area: adjacent cortical circuits and long-range white matter connections. Brain Lang 2013;125:146–55. [PubMed: 22632810]
69. Binder JR, Desai RH. The neurobiology of semantic memory. Trends Cogn Sci 2011;15:527–36. [PubMed: 22001867]
70. Ralph MA, Jefferies E, Patterson K, Rogers TT. The neural and computational bases of semantic cognition. Nat Rev Neurosci 2017;18:42–55. [PubMed: 27881854]
71. Joo SJ, Tavabi K, Caffarra S, Yeatman JD. Automaticity in the reading circuitry. Brain Lang 2021;214:104906. [PubMed: 33516066]
72. Kronbichler M, Hutzler F, Staffen W, Mair A, Ladurner G, Wimmer H. Evidence for a dysfunction of left posterior reading areas in German dyslexic readers. Neuropsychologia 2006;44:1822–32. [PubMed: 16620890]

73. Morken F, Helland T, Hugdahl K, Specht K. Reading in dyslexia across literacy development: A longitudinal study of effective connectivity. Neuroimage 2017;144:92–100. [PubMed: 27688204]
74. Maisog JM, Einbinder ER, Flowers DL, Turkeltaub PE, Eden GF. A meta-analysis of functional neuroimaging studies of dyslexia. Ann N Y Acad Sci 2008;1145:237–59. [PubMed: 19076401]
75. Grussu F, Schneider T, Tur C, et al. Neurite dispersion: a new marker of multiple sclerosis spinal cord pathology? Ann Clin Transl Neurol 2017;4:663–79. [PubMed: 28904988]
76. Fukutomi H, Glasser MF, Zhang H, et al. Neurite imaging reveals microstructural variations in human cerebral cortical gray matter. Neuroimage 2018;182:488–99. [PubMed: 29448073]
77. Im K, Raschle NM, Smith SA, Ellen Grant P, Gaab N. Atypical sulcal pattern in children with developmental dyslexia and at-risk kindergarteners. Cereb Cortex 2016;26:1138–48. [PubMed: 25576531]
78. Klein D, Rotarska-Jagiela A, Genc E, et al. Adolescent brain maturation and cortical folding: evidence for reductions in gyrification. PLoS One 2014;9:e84914. [PubMed: 24454765]
79. Lebel C, Deoni S. The development of brain white matter microstructure. Neuroimage 2018;182:207–18. [PubMed: 29305910]
80. Stevens WD, Kravitz DJ, Peng CS, Tessler MH, Martin A. Privileged functional connectivity between the visual word form area and the language system. J Neurosci 2017;37:5288–97. [PubMed: 28450544]
81. Lynch KM, Cabeen RP, Toga AW, Clark KA. Magnitude and timing of major white matter tract maturation from infancy through adolescence with NODDI. Neuroimage 2020;212:116672. [PubMed: 32092432]
82. Shaw P, Kabani NJ, Lerch JP, et al. Neurodevelopmental trajectories of the human cerebral cortex. J Neurosci 2008;28:3586–94. [PubMed: 18385317]
83. Raschle NM, Chang M, Gaab N. Structural brain alterations associated with dyslexia predate reading onset. Neuroimage 201;57:742–9.
84. Kostovic I, Vasung L. Insights from in vitro fetal magnetic resonance imaging of cerebral development. Semin Perinatol 2009;33:220–33. [PubMed: 19631083]
85. Meng Y, Li G, Lin W, Gilmore JH, Shen D. Spatial distribution and longitudinal development of deep cortical sulcal landmarks in infants. Neuroimage 2014;100:206–18. [PubMed: 24945660]
86. Grigorenko EL. Genetic bases of developmental dyslexia: A capsule review of heritability estimates. Enfance 2004;56:273–88.
87. Friedmann N, Coltheart M. Types of developmental dyslexia. In: Handbook of Communication Disorders De Gruyter Mouton, ed; 2018: 721–52
88. Goswami U Why theories about developmental dyslexia require developmental designs. Trends Cogn Sci 2003;7:534–40. [PubMed: 14643369]
89. Ramus F, Altarelli I, Jednoróg K, Zhao J, Scotto di Covella L. Neuroanatomy of developmental dyslexia: Pitfalls and promise. Neurosci Biobehav Rev 2018;84:434–52. [PubMed: 28797557]
90. Xia Z, Hancock R, Hoeft F. Neurobiological bases of reading disorder Part I: Etiological investigations. Lang Linguist Compass 2017;11:e12239. [PubMed: 28785303]
91. Jelescu IO, Veraart J, Adisetiyo V, Milla SS, Novikov DS, Fieremans E. One diffusion acquisition and different white matter models: how does microstructure change in human early development based on WMTI and NODDI? Neuroimage 2015;107:242–56. [PubMed: 25498427]
92. Jelescu IO, Veraart J, Fieremans E, Novikov DS. Degeneracy in model parameter estimation for multi-compartmental diffusion in neuronal tissue. NMR Biomed 2016;29:33–47. [PubMed: 26615981]
93. Kaden E, Kelm ND, Carson RP, Does MD, Alexander DC. Multi-compartment microscopic diffusion imaging. Neuroimage 2016;139:346–59. [PubMed: 27282476]

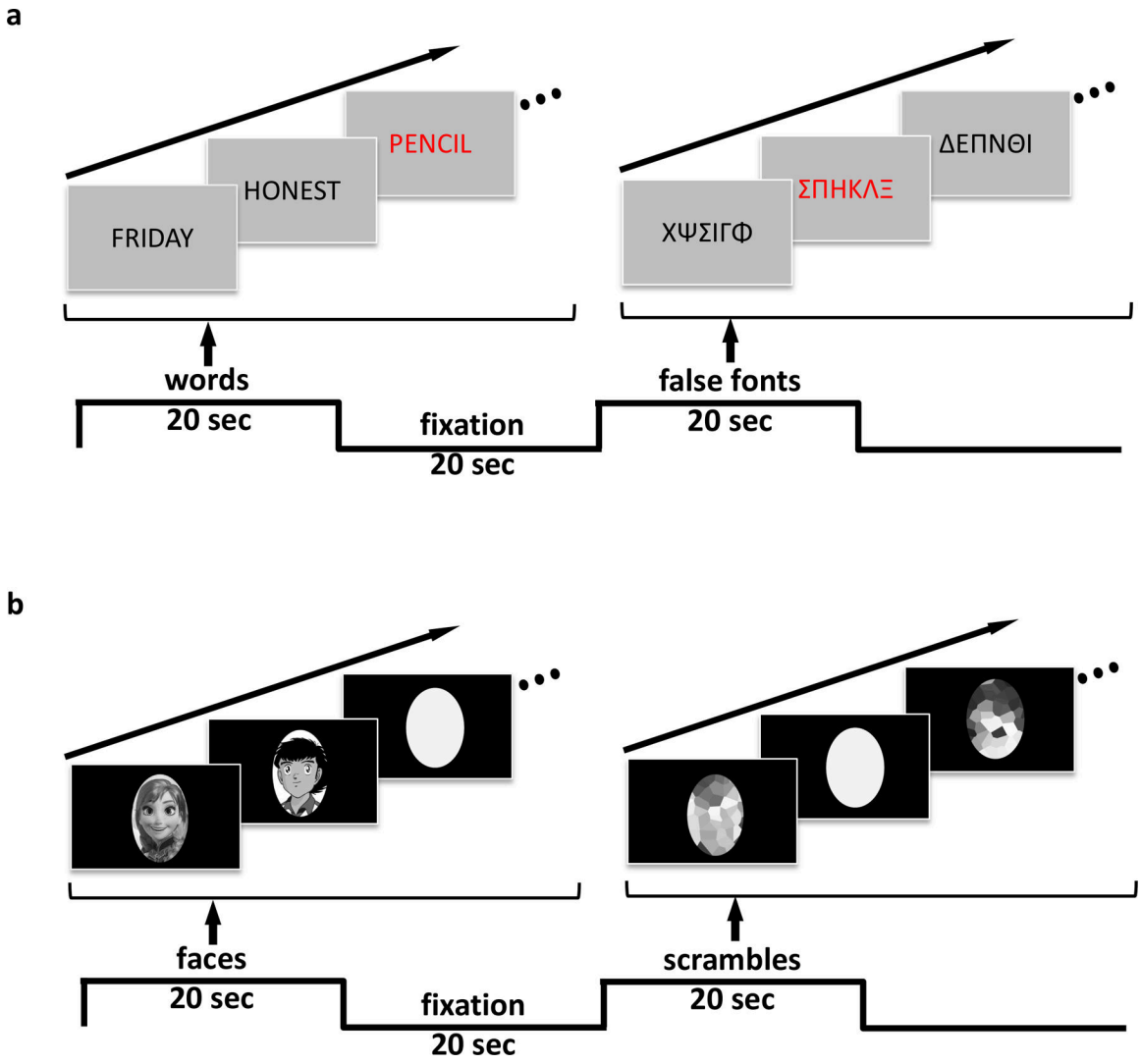

Figure 1. Experimental stimuli and task performed during the fMRI acquisition.

(a) Word task: participants are required to react to red stimuli in a flow of real English words or random strings of false fonts. (b) Face task: participants are presented with cartoon faces or scrambled images and have to detect the appearance of a blank oval.

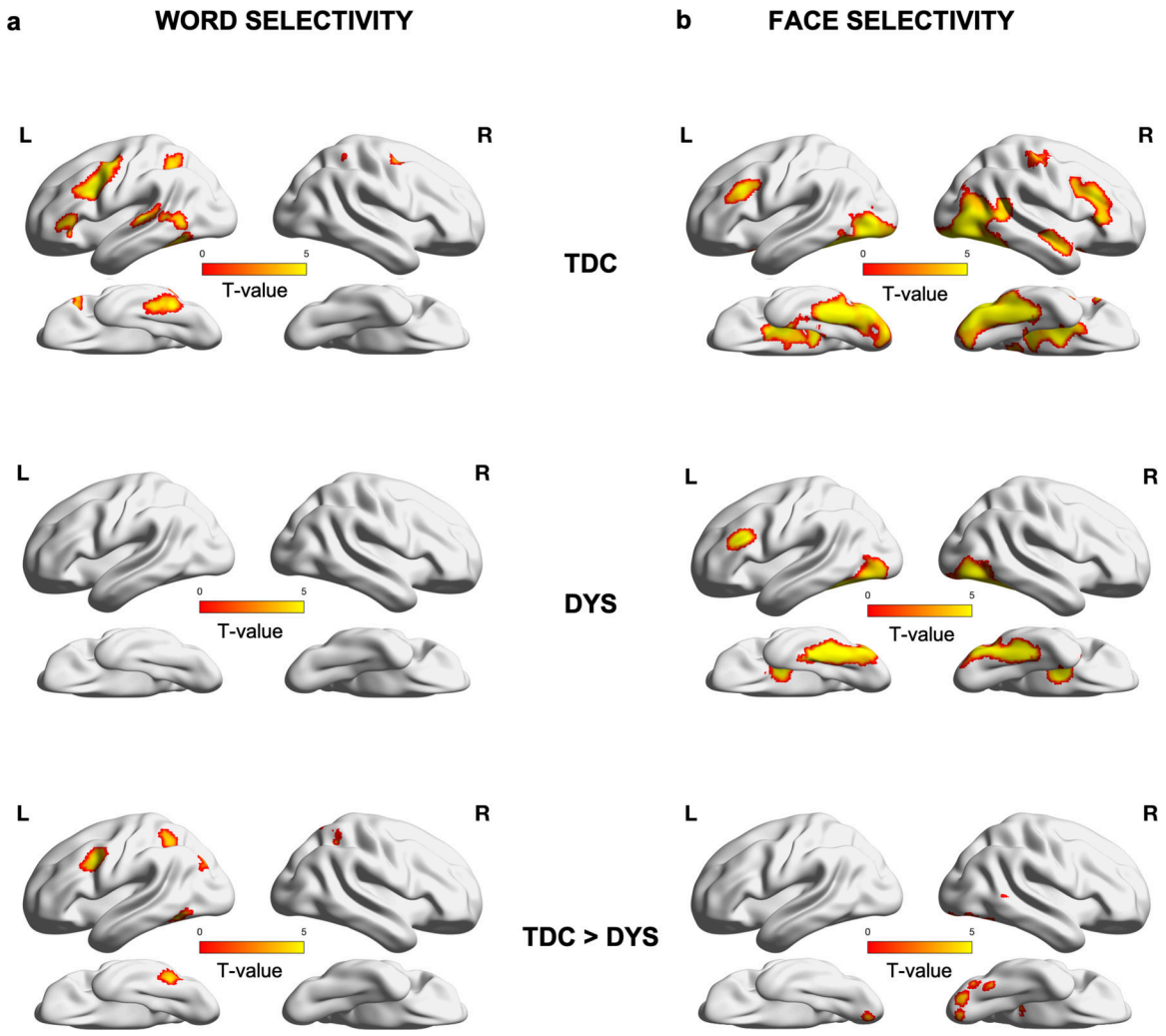

Figure 2. Whole-brain effects of fMRI tasks.

(a) Results of the contrast Words > False Fonts in typically developing controls (upper row, TDC), dyslexic (middle row, DYS), and their direct comparison (lower row, TDC > DYS). (b) Same as in (a) but for the contrast Faces > Scrambled Images. Plotted clusters are set at a threshold of $p < 0.001$ uncorrected with a cluster extent threshold of 100 voxels. **L = left hemisphere, R = right hemisphere.**

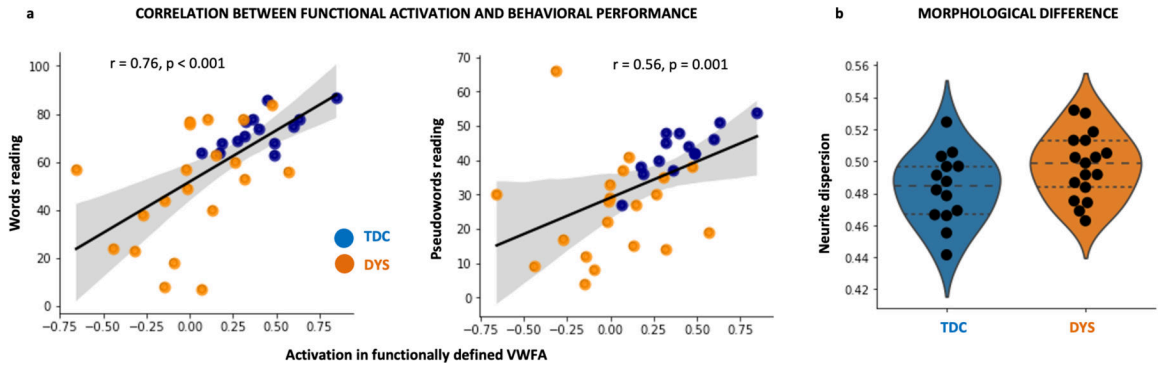

Figure 3. Morphological differences and behavioral correlates

(a) Correlation between the functional activation (BOLD signal) in the functionally defined visual word form area (VWFA) and behavioral performance during word reading (left plot, SWE raw scores) and pseudoword reading (right plot, PDE raw scores). Dots indicate individual subjects, blue = TDC, orange = DYS. (b) Neurite dispersion index in functionally defined VWFA in typically developing controls (TDC, blue) and children with dyslexia (DYS, orange).

Table 1:

Demographic and neuropsychological profiles of children with developmental dyslexia (DYS) and typically developing controls (TDC).

	Percentile scores		**p-value**
	DYS (N =26)	TDC (N =14)	
Age (years)	10.4 [2.0]	10.4 [1.6]	
WASI Matrix Reasoning	68.1 [25.3]	74.7 [15.6]	0.28
TOWRE SWE	20.0 [21.6] #30	58.7 [24.0]	<0.001
TOWRE PDE	17.2 [13.7] #30	61.0 [20.9]	<0.001
GORT Rate	26.6 [20.2] #21	N/A	N/A
GORT Accuracy	15.0 [14.1] #21	N/A	N/A
GORT Fluency	19.7 [14.3] #21	N/A	N/A
GORT Comprehension	28.6 [20.9] #21	N/A	N/A

Reading, oral language, and cognitive scores are reported in percentiles (mean **[standard deviation]**).

#denotes the number of children for which the score is available. WASI = Wechsler Abbreviated Scale of Intelligence; TOWRE= Test of Word Reading Efficiency; SWE= Sight Word Efficiency; PDE= Phonemic Decoding Efficiency; GORT = Gray Oral Reading Test. **N = number of participants; N/A = data not available.**

Table 2.

Significant clusters from within- and between-group analyses of the fMRI task.

Brain area	MNI coordinates			N voxels	P (FWE)	Max T
	x	y	z			
TDC: words > false fonts						
left superior frontal - BA 8	−40	10	32	1369	<0.001	6.83
left fusiform- BA 37	−46	−58	−18	663	0.001	6.69
left inferior frontal - BA 45	−40	34	0	292	0.02	5.49
left parietal - BA 7	−30	−46	46	271	0.04	5.37
TDC: faces > scrambled images						
right fusiform- BA 37	44	−66	−18	7341	<0.001	11
left fusiform- BA 37	−40	−56	−20	3598	<0.001	9.27
left superior temporal - BA 34	−28	0	−16	1460	<0.001	6.69
right superior frontal - BA 9	42	24	24	897	<0.001	5.27
left superior frontal - BA 9	−42	20	28	391	0.011	5.25
right primary sensory area	42	−20	48	413	0.009	5.01
DYS: words > false fonts						
no suprathreshold clusters						
DYS: faces > scrambled images						
right fusiform- BA 37	42	−42	−18	2822	<0.001	9.92
left fusiform- BA 37	−38	−38	−20	2683	<0.001	9.62
left superior frontal - BA 46	−48	32	20	353	0.017	5.88
Words: TDC >DYS						
left parietal - BA 7	38	−52	62	309	0.024	5.47
left fusiform- BA 37	−46	−58	−18	404	0.008	5.36
left superior frontal - BA 8	−42	8	36	361	0.013	5.29
Faces: TDC > DYS						
right fusiform- BA 37	44	−68	−18	503	0.003	4.92
Words: DYS > TDC						
no suprathreshold clusters						
Faces: DYS > TDC						
no suprathreshold clusters						

MNI = Montreal Neurological Institute coordinate space ; FWE = Family Wise Error correction; BA = Brodmann Area